

Transport mechanisms of intracellular metabolites in the brain: new insights by diffusion-weighted NMR spectroscopy with oscillating gradients

Charlotte Marchadour^{1,2}, Vincent Lebon^{1,2}, and Julien Valette^{1,2}

¹CEA-MIRCen, Fontenay-aux-Roses, France, ²CEA-CNRS URA 2210, Fontenay-aux-Roses, France

Introduction:

Transport of molecules within cells is a key process in cellular biology. Transport can be achieved either passively by random diffusion, or by active transport, including specific molecular motors conveying cargos, or general convection of the cytosol (known as cytoplasmic streaming or cyclosis). The relative contribution of passive and active transport mechanisms to the apparent diffusion coefficient (ADC) of intracellular metabolites and intracellular water is still debated. As a matter of fact, many works have invoked failure of energy-dependent active transport, in particular cytoplasmic streaming, as a possible explanation for the observed massive ADC drop of brain intracellular molecules observed in ischemic stroke (eg. [1-4]). In the present work, we investigate metabolite motion in the rat brain *in vivo* using an original diffusion-weighted NMR spectroscopy (DW-MRS) approach using oscillating gradients. With this strategy, the temporal dependence of brain metabolite ADC is observed for the first time, for diffusion frequency ω_d ranging from 19 Hz to 267 Hz (corresponding to diffusion time t_d ranging from ~1 ms to ~13 ms). Exploiting the unique ability of oscillating gradients to probe the motion spectrum, it appears that random diffusion is the dominant transport mechanism for intracellular metabolites in the living brain. Armed with this knowledge, we perform data modeling based on geometrically constrained diffusion. Estimated parameters are consistent with known cellular architecture, further ruling out the plausibility of significant active transport.

Theory:

A powerful framework for the study of molecular motion is the formalism of velocity autocorrelation function $VAF(t) = \langle v(0)v(t) \rangle$, where $v(t)$ is the speed of an individual molecule along the magnetic field gradient direction at time t , and $\langle \rangle$ stands for the ensemble average. For hindered random diffusion, $VAF(t) \rightarrow 0$ for $t > 0$ whereas for active transport, $VAF(t) > 0$ for $t > 0$. In both cases, loss of motion coherence in the long-time tail makes VAF smoothly converge to 0 as t increases. One way to characterize the VAF is the study of the motion spectrum $D(\omega)$, which is its Fourier transform. Negative VAF corresponds to $D(\omega)$ increasing at higher ω while positive VAF corresponds to $D(\omega)$ decreasing at higher ω [5]. Apodized cosine-modulated diffusion-weighting gradients [6] allow sampling $D(\omega)$ at very specific "diffusion frequencies" $\omega_d \sim N/T$, T being the duration of the gradient and N the number of periods during T . For a given gradient waveform, it can be shown that signal attenuation is equal to $\exp(-bD(\omega_d))$, with b the usual time integral of the square of the gradient moment, so that ADC as measured by log-linear regression is equal to $D(\omega_d)$. Correspondence with the time domain, although only approximate, is achieved using $t_d = 0.25/\omega_d$ [6].

Materials and methods:

NMR setup: Experiments were performed on a Varian 7 T scanner equipped with a rodent gradient coil reaching 600 mT/m along each axis. RF transmission was performed using a birdcage coil while reception was achieved with a quadrature surface coil with integrated preamplifiers.

DW-spectroscopy: Two cosine-modulated gradients were inserted in a LASER sequence (TE/TR=154/2000 ms) on both sides of the first 180°. For each gradient $T=60$ ms, and N varied from 1 to 16, corresponding to effective ω_d ranging from 19.3 to 267 Hz as calculated by Fourier transform and numerical integration of the effective gradient moment. This corresponds to t_d ranging from 0.94 to 13 ms. Gradient amplitude was adjusted to get $b=1000$ s/mm² for every ω_d .

Experiments: Spectra were acquired in a large voxel (450 μ L) in the brain of healthy Sprague-Dawley rats (Fig. 1A). Twenty scanning sessions were performed. Each session consisted in acquiring water reference spectra (1 average) and metabolite spectra (128 averages) at $b=0$ and at $b=1000$ s/mm² for six values of ω_d .

Data processing: Water spectra were used to measure water ADC and to correct for eddy currents on metabolite spectra. No phase variation was observed between individual scans, so spectra were simply summed before quantification by LCModel [7]. Finally, ADC was calculated for the most reliably quantified metabolites: N-acetylaspartate (NAA), total choline (tCho) and total creatine (tCr).

Diffusion models: ADC averaged over the three metabolites was fitted using two models of restricted diffusion based on the theoretical expression of $D(\omega_d)$ as given by Stepišnik [5]. The first model consisted in hollow cylinders isotropically oriented in 3D, to account for diffusion in long fibers ("neurite model"); unknown parameters were the free diffusion coefficient D_{free} and the fiber diameter d . Second model consisted in interconnected spherical pores to account for diffusion in the tortuous internum of large cell bodies filled with organelles ("cell body model"); unknown parameters were D_{free} , the pore diameter d and the tortuosity T .

Results and discussion:

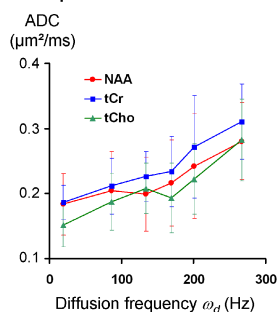
High quality spectra could be obtained, with eye-visible dependence of signal attenuation during single scanning sessions (Fig. 1B). At shorter ω_d (longer t_d), metabolite ADC is close to results already published ($ADC_{NAA}=0.18$ $\mu\text{m}^2/\text{ms}$, $ADC_{tCr}=0.15$ $\mu\text{m}^2/\text{ms}$, $ADC_{tCho}=0.19$ $\mu\text{m}^2/\text{ms}$). ADC increased at higher ω_d (Fig. 2A), with a 50% increase for NAA, 80% for tCho and 60% for tCr between lowest and highest ω_d . In contrast, experiments on phantom exhibited stable ADC. ADC increase corresponds to negative VAF, demonstrating the dominance of hindered random diffusion on these time-scales. This justifies the use of models based on geometrically restricted diffusion, which both account well for measured ADC (Fig. 2B). For the "neurite model", best fit yielded $D_{free}=0.5$ $\mu\text{m}^2/\text{ms}$ and $d=2$ μm , which is consistent with typical diameter of axons, dendrites and other fibers such as astrocytic processes. For the "cell body model", best fit yielded $D_{free}=0.6$ $\mu\text{m}^2/\text{ms}$, $T=1.9$, and $d=2$ μm , consistently with the typical size of and distance between organelles. In both models D_{free} is ~20% lower than in free water, which agrees with the low fluid-phase viscosity of the cytoplasm as measured through rotational correlation times [8]. The consistency of estimated parameters, without invoking active transport, reinforces the idea that random diffusion is the main transport mechanism. Note that extending both models to longer t_d , using

the numerical values for D_{free} , R and T as determined here, accounts well for the apparent stability of brain metabolite ADC in the literature over t_d ranging from 13 ms [2] to 224 ms [9]. Determining if the actual diffusion compartment of brain metabolites is closer to the neurite or the cell body model requires going to ultra-long t_d , as shown in another work [Najac *et al.*, this symposium].

Conclusion:

Using an original DW-MRS sequence, we reported the first *in vivo* observation of the time-dependence of brain metabolite ADC. The interpretation of our results in terms of velocity autocorrelation function, made possible by the use of oscillating gradients, and further reinforced by data modeling based exclusively on geometrically constrained random diffusion, establishes solid grounds for random diffusion being the dominant transport mechanism of brain metabolites, leaving only little room for significant active transport.

A. Experimental data



B. Data fit

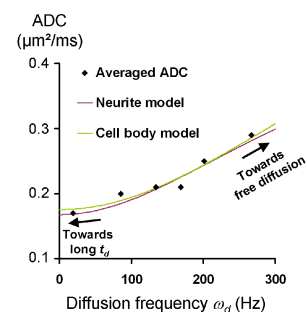


Figure 2: A) Metabolite ADC as a function of ω_d . B) ADC averaged for the three metabolites, and the best fit for the neurite and cell body models.

[1] Neil MRM 1996; [2] Dreher MRM 2001; [3] Ackerman NMR Biomed 2010; [4] Harkins MRM 2011; [5] Stepišnik Physica 1993; [6] Does MRM 2003; [7] Provencher MRM 1993; [8] Verkman Trends Biochem Sci 2002 [9] Posse Radiology 1993.